Electronic Supplementary Information for…

Protonation Induces Base Rotation of Purine Nucleotides pdGuo and pGuo

R. R. Wu,[†] C. C. He,[†] L. A. Hamlow,[†] Y.-w. Nei,[†] G. Berden,[‡] J. Oomens,[‡§] and M. T. Rodgers[†,*]

[†]*Department of Chemistry, Wayne State University, Detroit, Michigan 48202*
[‡]*FELIX Laboratory, Institute for Molecules and Materials, Radboud University, Toernooiveld 7, 6525ED, Nijmegen, The Netherlands,*
[§]*van't Hoff Institute for Molecular Sciences, University of Amsterdam, 1090 GD Amsterdam, The Netherlands*

Discussion

Comparison of Experimental IRMPD and Theoretical IR Spectra of [pdGuo+H]$^+$. The measured IRMPD and calculated IR spectra of the **N7B**, **N7D**, **O6B** and **N3a** of [pdGuo+H]$^+$ are compared in Figure S3 over the IR fingerprint and hydrogen-stretching regions. Mismatches between the measured and calculated spectra are highlighted. Both calculated IR spectra of N7 protonated conformers, **N7B** and **N7D**, exhibit good agreement with the measured spectrum in the IR fingerprint region, whereas the calculated IR spectra of the O6 and N3 protonated conformers again exhibit obvious disagreement with the measured spectrum in the IR fingerprint region, particularly above ~1500 cm^{-1}. In the hydrogen-stretching region, the calculated IR spectra of all four conformers exhibit disagreement with the measured IR spectrum. The IR feature predicted at ~3680 cm^{-1} for **N7B** broadens the calculated band at ~3645 cm^{-1}, which is lower in frequency than the band observed at ~3660 cm^{-1}. Similarly, the calculated band at ~3645 cm^{-1} for **N7D** is lower in frequency than the band observed at ~3660 cm^{-1}. The calculated bands at ~3575 cm^{-1} for **O6B**, and ~3540 cm^{-1} for **N3a** are higher and lower in frequency, respectively, than the measured band at ~3565 cm^{-1}. The calculated bands at ~3440 and ~3430 cm^{-1} for **O6B** and **N3a** are lower in frequency than the measured band at ~3455 cm^{-1}. Therefore, the **N7B**, **N7D**, **O6B** and **N3a** conformers are not populated in the experiments.

Comparison of Experimental IRMPD and Theoretical IR Spectra of [pGuo+H]$^+$. The measured IRMPD and calculated IR spectra of the **N7B**, **N7i**, **N7ii** and **N7iii** conformers of [pGuo+H]$^+$ are compared in Figure S4 over the IR fingerprint and hydrogen-stretching regions. The calculated IR spectra of these four N7 protonated conformers all exhibit good agreement with the measured spectrum in the IR fingerprint region. However, mismatches are observed for all of these conformers in the hydrogen-stretching regions, and are highlighted in the figure. The hydrogen-bond acceptor O3'H stretching predicted at ~3680 cm^{-1} for **N7B** is again not diagnostic due to the O2'H···O3' hydrogen-bonding interaction. The calculated bands at ~3645 and ~3580 cm^{-1} for **N7B** are lower and higher in frequency than the measured bands at ~3660 and ~3580 cm^{-1}, respectively. The calculated bands at ~3620 cm^{-1} for **N7i**, ~3600 cm^{-1} for **N7ii**, and ~3620 and ~3520 cm^{-1} for **N7iii**, are all not observed in the measured spectrum. Therefore, these four N7 protonated conformers are absent from the experimental population.

The measured IRMPD and calculated IR spectra of the **N7D**, **O6B** and **N3i** conformers of [pGuo+H]$^+$ in the IR fingerprint and hydrogen-stretching regions are compared in Figure S5 with mismatches again highlighted. In the IR fingerprint region, the calculated spectrum of the N7 protonated **N7D** conformer exhibits good agreement with

the measured spectrum, whereas those of the O6 and N3 protonated conformers, **O6B** and **N3i**, exhibit obvious discrepancies with the measured spectrum. In the hydrogen-stretching region, the calculated spectra of all three conformers exhibit evident disagreement with the measured spectrum. Therefore, the **N7D**, **O6B** and **N3i** conformers are also not populated in the experiments.

Figure Captions

Figure S1. B3LYP/6-311+G(d,p) low-energy conformers of $[pdGuo+H]^+$ and their relative Gibbs free energies at 298 K calculated at the B3LYP/6-311+G(2d,2p) (in black) and MP2(full)/6-311+G(2d,2p) (in red) levels of theory. The site of protonation, nucleobase orientation, and sugar puckering are also indicated for each conformer.

Figure S2. B3LYP/6-311+G(d,p) low-energy conformers of $[pGuo+H]^+$ and their relative Gibbs free energies at 298 K calculated at the B3LYP/6-311+G(2d,2p) (in black) and MP2(full)/6-311+G(2d,2p) (in red) levels of theory. The site of protonation, nucleobase orientation, and sugar puckering are also indicated for each conformer.

Figure S3. Comparison of the measured IRMPD action spectrum of $[pdGuo+H]^+$ with the theoretical linear IR spectra of the **N7B**, **N7D**, **O6B** and **N3a** conformers of $[pdGuo+H]^+$ and the corresponding B3LYP/6-311+G(d,p) optimized structures. Also shown are the B3LYP/6-311+G(2d,2p) (in black) and MP2(full)/6-311+G(2d,2p) (in red) relative Gibbs free energies at 298 K. The site of protonation, nucleobase orientation, and sugar puckering are also indicated for each conformer. To facilitate comparison of the measured and computed spectra, the IRMPD spectrum is overlaid (in grey) with each computed spectrum and scaled to match the intensity of the most intense feature in each region.

Figure S4. Comparison of the measured IRMPD action spectrum of $[pGuo+H]^+$ with the theoretical linear IR spectra of the **N7B**, **N7i**, **N7ii** and **N7iii** conformers of $[pGuo+H]^+$ and the corresponding B3LYP/6-311+G(d,p) optimized structures. Also shown are the B3LYP/6-311+G(2d,2p) (in black) and MP2(full)/6-311+G(2d,2p) (in red) relative Gibbs free energies at 298 K. The site of protonation, nucleobase orientation, and sugar puckering are also indicated for each conformer. To facilitate comparison of the measured and computed spectra, the IRMPD spectrum is overlaid (in grey) with each computed spectrum and scaled to match the intensity of the most intense feature in each region.

Figure S5. Comparison of the measured IRMPD action spectrum of $[pGuo+H]^+$ with the theoretical linear IR spectra of the **N7D**, **O6B** and **N3i** conformers of $[pGuo+H]^+$ and the corresponding B3LYP/6-311+G(d,p) optimized structures. Also shown are the B3LYP/6-311+G(2d,2p) (in black) and MP2(full)/6-311+G(2d,2p) (in red) relative Gibbs free energies at 298 K. The site of protonation, nucleobase orientation, and sugar puckering are also indicated for each conformer. To facilitate comparison of the measured and computed spectra, the IRMPD spectrum is overlaid (in grey) with each computed spectrum and scaled to match the intensity of the most intense feature in each region.

Figure S1.

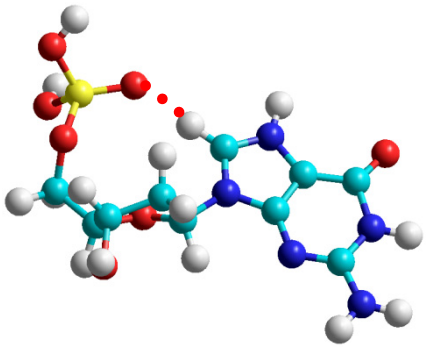

N7A, anti, C2'-endo
0.0, 0.0 kJ/mol

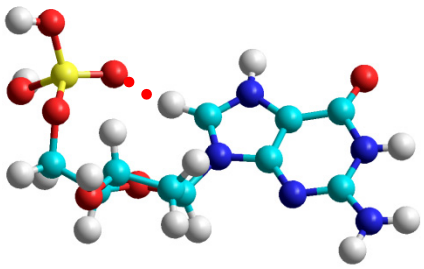

N7B, anti, C3'-endo
2.2, 4.2 kJ/mol

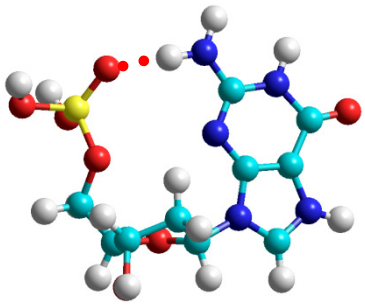

N7C, syn, C2'-endo
13.5, 4.5 kJ/mol

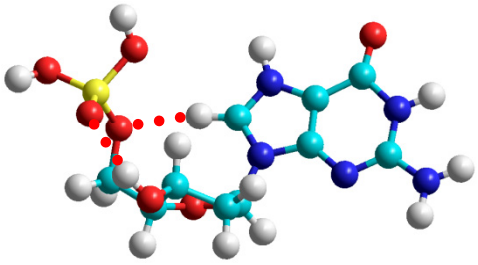

N7D, anti, C3'-endo
13.7, 1.8 kJ/mol

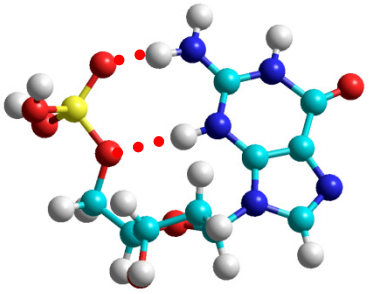

N3A, syn, C2'-endo
32.5, 16.9 kJ/mol

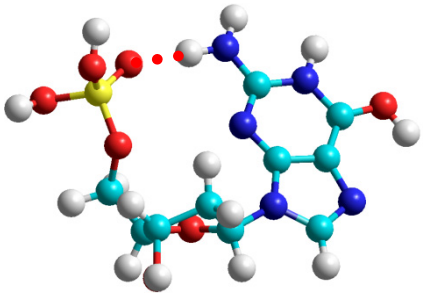

O6A, syn, C2'-endo
45.7, 37.9 kJ/mol

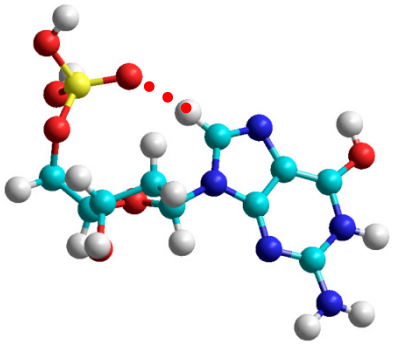

O6B, anti, C2'-endo
50.0, 47.5 kJ/mol

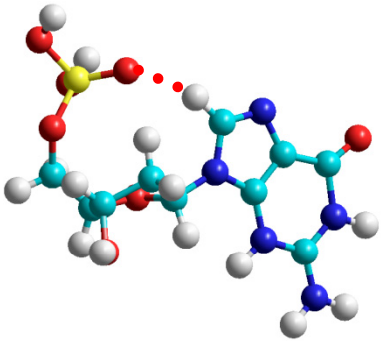

N3a, anti, C2'-endo
95.7, 85.7 kJ/mol

$[pdGuo+H]^+$

Figure S2.

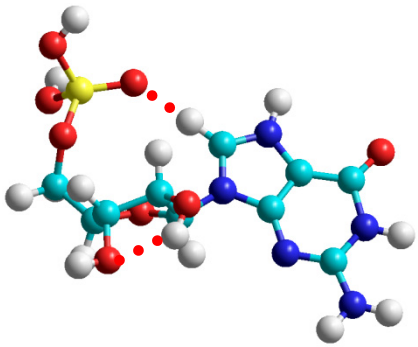

N7A, anti, C2'-endo
0.0, 0.0 kJ/mol

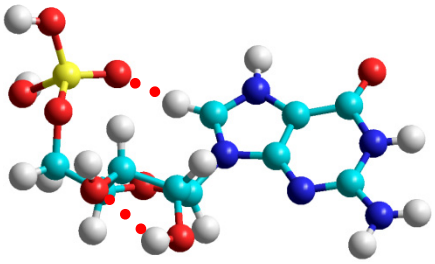

N7B, anti, C3'-endo
4.9, 4.8 kJ/mol

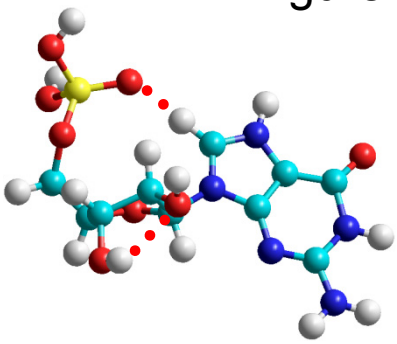

N7i, anti, C2'-endo
5.0, 2.7 kJ/mol

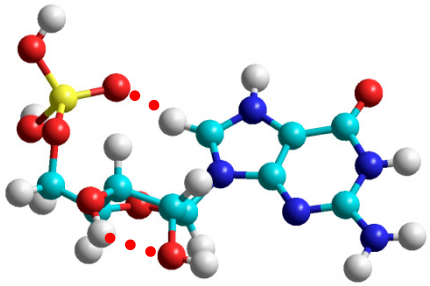

N7ii, anti, C3'-endo
10.1, 9.8 kJ/mol

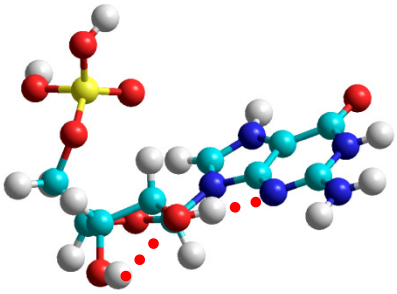

N7iii, anti, C2'-endo
11.4, 3.4 kJ/mol

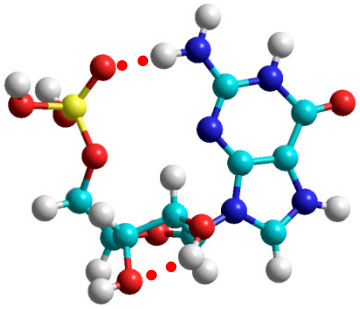

N7C, syn, C2'-endo
12.9, 4.7 kJ/mol

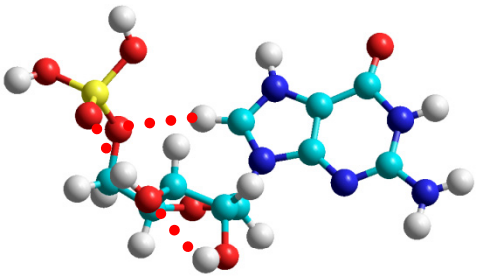

N7D, anti, C3'-endo
14.6, 2.1 kJ/mol

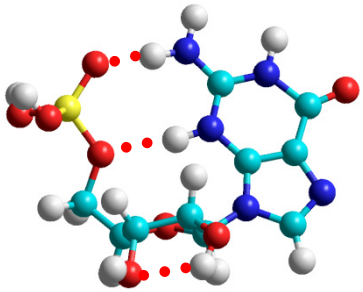

N3A, syn, C2'-endo
37.6, 23.4 kJ/mol

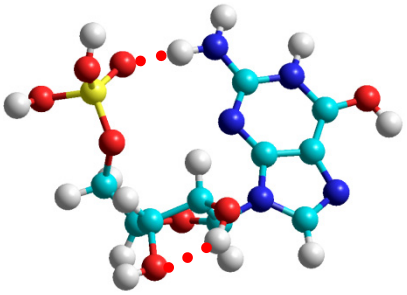

O6A, syn, C2'-endo
44.9, 38.0 kJ/mol

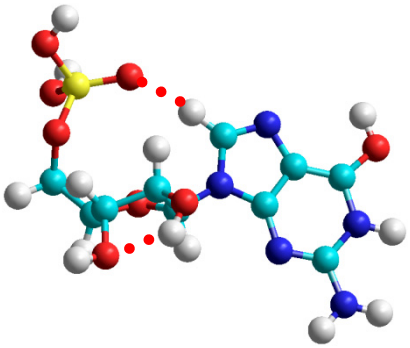

O6B, anti, C2'-endo
47.9, 46.3 kJ/mol

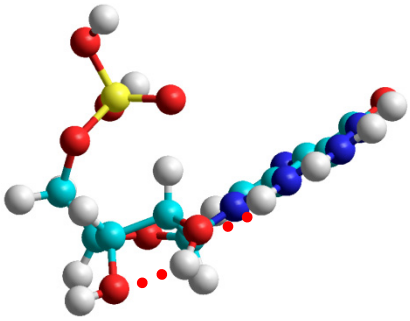

N3i, anti, C2'-endo
68.4, 43.7 kJ/mol

[pGuo+H]$^+$

Figure S3.

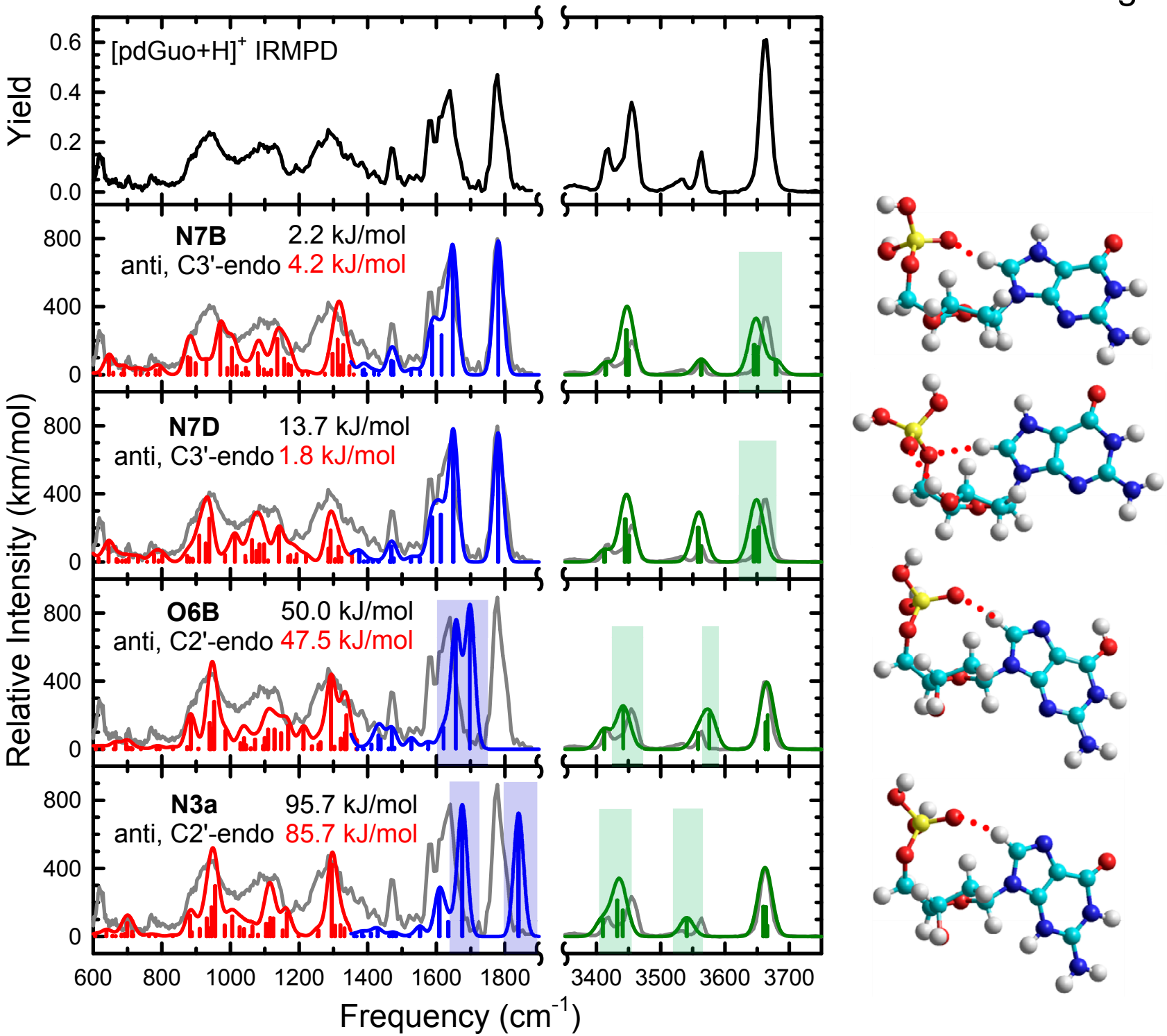
[pdGuo+H]+ IRMPD
Yield
0.6
0.4
0.2
0.0
N7B 2.2 kJ/mol
anti, C3'-endo 4.2 kJ/mol
N7D 13.7 kJ/mol
anti, C3'-endo 1.8 kJ/mol
O6B 50.0 kJ/mol
anti, C2'-endo 47.5 kJ/mol
N3a 95.7 kJ/mol
anti, C2'-endo 85.7 kJ/mol
Relative Intensity (km/mol)
800
400
0
600 800 1000 1200 1400 1600 1800
3400 3500 3600 3700
Frequency (cm-1)

Figure S4.

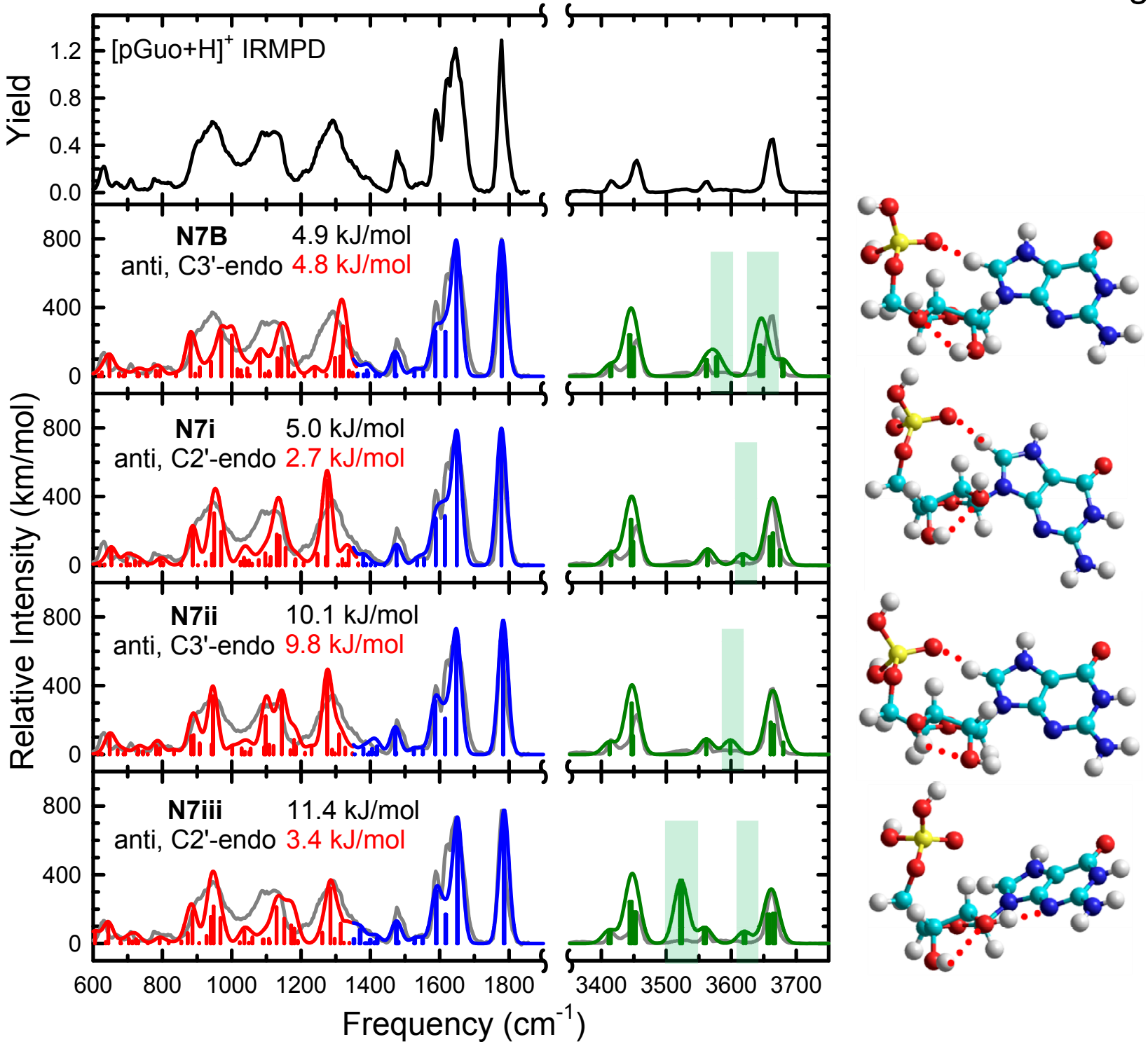
[pGuo+H]+ IRMPD
Yield
1.2
0.8
0.4
0.0
N7B 4.9 kJ/mol
anti, C3'-endo 4.8 kJ/mol
N7i 5.0 kJ/mol
anti, C2'-endo 2.7 kJ/mol
N7ii 10.1 kJ/mol
anti, C3'-endo 9.8 kJ/mol
N7iii 11.4 kJ/mol
anti, C2'-endo 3.4 kJ/mol
Relative Intensity (km/mol)
800
400
0
600 800 1000 1200 1400 1600 1800
3400 3500 3600 3700
Frequency (cm-1)

Figure S5.

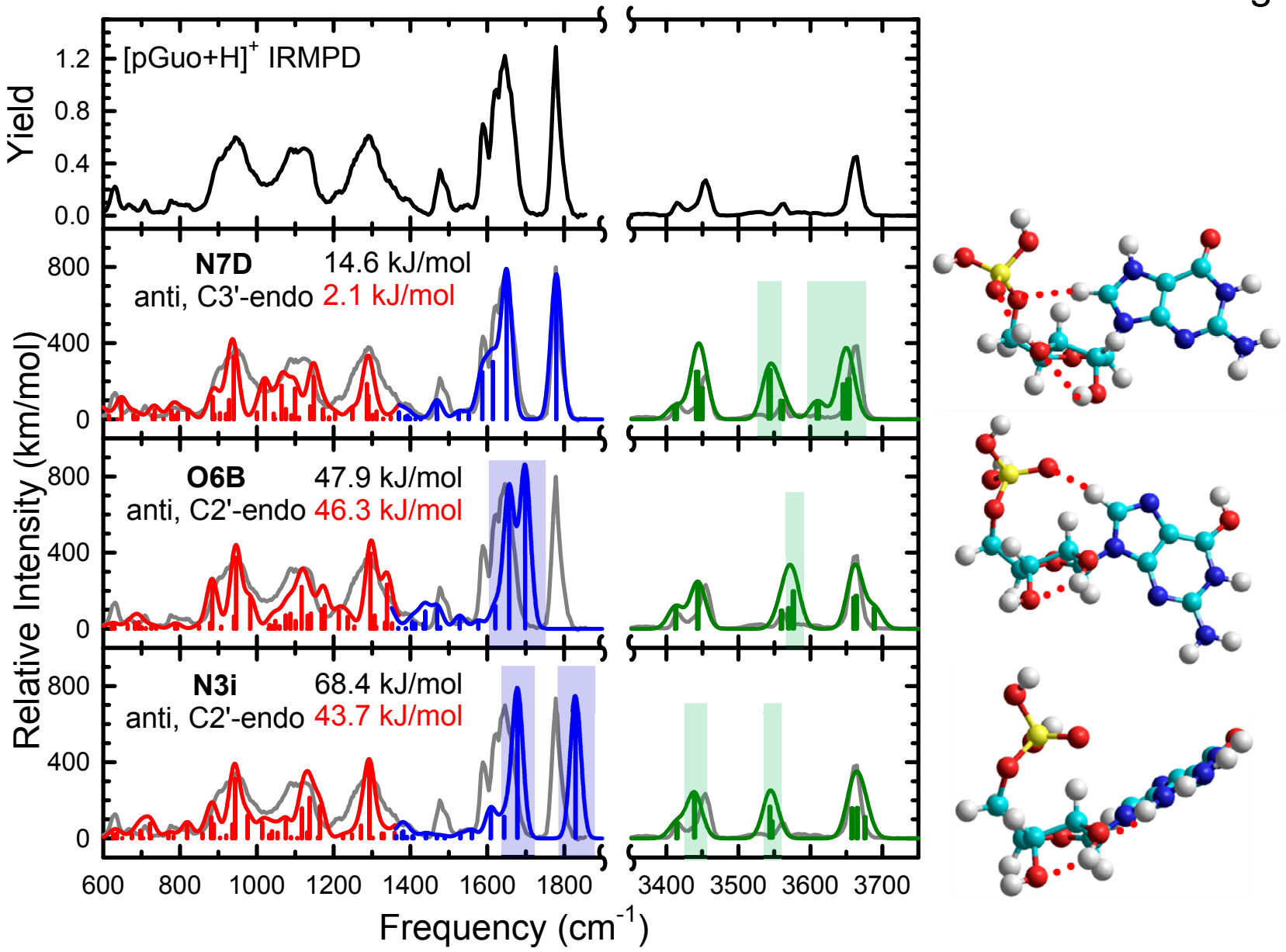
[pGuo+H]+ IRMPD
Yield
1.2
0.8
0.4
0.0
N7D
14.6 kJ/mol
anti, C3'-endo 2.1 kJ/mol
O6B
47.9 kJ/mol
anti, C2'-endo 46.3 kJ/mol
N3i
68.4 kJ/mol
anti, C2'-endo 43.7 kJ/mol
Relative Intensity (km/mol)
800
400
0
600
800
1000
1200
1400
1600
1800
3400
3500
3600
3700
Frequency (cm-1)